Grid Refinement in Cartesian Coordinates for Groundwater Flow Models Using the Divergence Theorem and Taylor's series.

Mansour M.M. and Spink A.E.F.

Abstract

Grid refinement is introduced in a numerical groundwater model to increase the accuracy of the solution over local areas without compromising the run time of the model. Numerical methods developed for grid refinement suffered certain drawbacks, for example deficiencies in the implemented interpolation technique; the non-reciprocity in head calculations or flow calculations; lack of accuracy resulting from high truncation errors, and numerical problems resulting from the construction of elongated meshes. A refinement scheme based on the divergence theorem and Taylor's expansions is presented here. This scheme is based on the work of De Marsily (1986) but includes more terms of the Taylor's series to improve the numerical solution. In this scheme flow reciprocity is maintained and high order of refinement was achievable. The new numerical method, investigated by modelling flows in homogeneous confined aquifers, produced results with acceptable degrees of accuracy. It converges and reproduces the desired solution in heterogeneous aquifers. This method also shows the potential for application to solving groundwater heads over nested meshes with irregular shapes.

Introduction

The finite difference technique is a numerical method that is used to solve the differential equation representing the spatial and temporal variations of the groundwater heads of groundwater systems. Like other numerical techniques, for example, the subsurface flow finite element models FEHM (Zyvoloski et al., 1997) and FEFLOW (Diersch, 2005), the continuous aquifer domain is discretised into a set of sub-domains or nodes, where groundwater heads are calculated. The increased number of nodes both improves the accuracy of the numerical solution and improves the processing time required to produce the solution. In the early days of finite difference applications, computational resources were limited in terms of both storage capacity and computational speed. This made the efficiency of a numerical method an important feature and most often the resolution of the numerical grids holding nodes was compromised to benefit run time. Today, storage capacity imposes few restrictions and computer speed is ever-increasing allowing more complicated and accurate numerical methods to be applied. However, the complexity of groundwater applications is increasing in parallel with the development of computer abilities and this has led researchers, for example Szekely (1998), Hayes(1999), Jackson (2000), Mehl and Hill (2004), Mehl et al. (2006), Dickinson et al. (2007), Szekely (2008) to continue to work on the development of numerical applications that satisfy both speed and accuracy.

The speed of solving a groundwater problem is mainly controlled by the power of the processor and by the number of nodes included in the numerical model. The accuracy of the solution, on the other hand, depends on many factors. A major factor is the spacing between adjacent nodes of the numerical grid. This affects the truncation error introduced into the numerical approximations and the accuracy of the representation of the rate of change of groundwater head over distance. A smooth change in the hydraulic gradient, as is the case in regional aquifers, for example, allows the use of a large interval without affecting the accuracy of the solution. In radial flow modelling, for example Rushton and Redshaw (1979) or Mansour et al. (2011), the use of a logarithmic radial mesh increases the node density in the region around the well where steep hydraulic gradients occur and reduces the node density in the more distant parts of the aquifer. However, steep hydraulic gradients may occur in a regional aquifer due to the existence of special features, such as rivers, wells, faults, and changes in the aquifer properties. This requires the use of a small space interval over these limited areas. Mesh refinement is a useful technique that increases the accuracy of the model without limiting its run-time efficiency or increasing computer memory.

Mesh refinement techniques were investigated as early as 1946 (Southwell, 1946) and different mesh refinement schemes have been developed over the years. For example telescopic refinement schemes with multiple scale models are used by Ward et al. (1987), Bravo et al. (1996) and Miller and Voss (1987), adaptive mesh refinement schemes are used by Berger and Oliger (1984), Arney and Flaherty (1989) and De Lange and De Goey (1994) and local grid refinement schemes are used by Szekeley (1998), Bennet and Smooke (1999), Hayes (1999), Jackson (2000) and Mehl et al. (2006). These methods successfully served the needs of their users giving acceptable accuracy for the type of problem investigated. However, each of these methods suffers from certain drawbacks, for example deficiencies in the implemented interpolation technique, lack of accuracy resulting from high truncation errors, and numerical problems resulting from the construction of elongated meshes. Other methods do not maintain grid reciprocity, which specifies that if point A is included in the finite difference approximation at point B, then point B must be included in the approximation at point A. If reciprocity exists then the approximation of flux leaving A and entering B can be formulated in exactly the same way as the approximation of the flux leaving B and entering A (Jackson, 2000; Mehl et al., 2006). De Marsily et al. (1978) present a refinement scheme based on integrated finite differences that has certain attractions. This scheme uses the Green Theorem to calculate the groundwater flows at the sides of the nodes located at the coarse-fine grid interfaces. It fits, therefore, neatly within the conventional finite differences and maintains a flow balance. However, the one drawback of the method as presented by De Marsily (1986) is its limited accuracy.

Jackson (2000) developed equations that are more accurate than De Marsily et al. (1978) and De Marsily (1986) although they do not maintain flow reciprocity. The lack of accuracy in the scheme developed by De Marsily (1986) originates from limiting the number of terms in the Taylor's series used to develop the numerical equations to just three, i.e. the heads and first gradients of heads.

This paper presents a refinement scheme based on the refinement scheme developed by De Marsily (1986) but improved by including more terms of the Taylor's series to derive the necessary numerical equations. The challenges of this are first to produce numerical equations that have the desired groundwater equation forms as the product of head differences multiplied by conductance parameters and second that the developed numerical technique is stable and converges to the required solution with an acceptable degree of accuracy. This paper discusses the steps required to derive the numerical equations and presents the grid discretisation scheme that reduces the effort required to derive these equations. The convergence of the numerical scheme is demonstrated by simulating groundwater flows in one and two dimensional homogeneous aquifers under steady state conditions. The convergence of the numerical scheme in transient problems is demonstrated by comparing the numerical results to the Theis solution. Finally the limitations of the method and recommendation for future development are discussed.

Description of the Methods

Integrated Finite Differences.

The basic flow equation in an anisotropic and heterogeneous aquifer is given by:

$$\frac{\partial}{\partial x}\left(T_x \frac{\partial h}{\partial x}\right)+\frac{\partial}{\partial y}\left(T_y \frac{\partial h}{\partial y}\right)=S\frac{\partial h}{\partial t}-q \qquad \text{Equation 1}$$

De Marsily et al. (1978) introduced the integrated finite difference technique based on the Divergence Theorem, or Green's Theorem. In two dimensions, the Divergence Theorem states that for any continuous vector function **V** with continuous first partial derivatives, the double integral of the divergence of this function over a closed area A can be transformed into a contour integral of the scalar product of the vector function with the unit outward normal evaluated along the perimeter C of the area A. This is expressed by, for example Boas (1983), De Marsily et al. (1978):

$$\iint_A div(\boldsymbol{V})\,dA = \oint_C \boldsymbol{V}\cdot\boldsymbol{n}\,ds \qquad \text{Equation 2}$$

To generalise the method, De Marsily (1986) considered an anisotropic aquifer and constructed a mesh where the grid elements have a polygonal shape with nodes located within them. In a conventional finite difference approximation, Equation 1 would be written at each of the nodes. In integrated finite differences, the integral of the flow equation over the area A_i surrounding each node is formed. This leads to:

$$\iint_A \left[\frac{\partial}{\partial x}\left(T_x \frac{\partial h}{\partial x}\right)+\frac{\partial}{\partial y}\left(T_y \frac{\partial h}{\partial y}\right)\right]da=\iint_A\left(S\frac{dh}{dt}-q\right)da \qquad \text{Equation 3}$$

and by recognising that the left hand side is a divergence term Equation 3 can be written as:

$$\iint_A div\left(T\ grad\, h\right)da=\iint_A\left(S\frac{dh}{dt}-q\right)da \qquad \text{Equation 4}$$

Finally the divergence theorem allows the left-hand side to be replaced by a line integral:

$$\oint_{\tau_i} \left(T_x \frac{\partial h}{\partial x} n_x + T_y \frac{\partial h}{\partial y} n_y \right) ds = \iint_A \left(S \frac{dh}{dt} - q \right) da \qquad \text{Equation 5}$$

Where n_x and n_y are the direction cosines of the unit vector **n** perpendicular to the boundary, and ds is an element of τ_I, the boundary of the element surrounding the node. As a result of this transformation, numerical approximations to $\frac{\partial h}{\partial x}$ and $\frac{\partial h}{\partial x}$ are required rather than to $\frac{\partial^2 h}{\partial x^2}$ and $\frac{\partial^2 h}{\partial x^2}$.

To evaluate the hydraulic gradients $\frac{\partial h}{\partial x}$ and $\frac{\partial h}{\partial x}$ at an arbitrary point (m) moving along line AB (Figure 1), De Marsily (1986) wrote three Taylor's series expansions for the head values at I, J and K. Only three terms of the Taylor's series are retained, as shown in Equation 6, allowing the gradients $\left.\frac{\partial h}{\partial x}\right|_m$ and $\left.\frac{\partial h}{\partial y}\right|_m$ at the point m to be calculated in terms of the heads at the surrounding nodes and their positions.

$$h_I = h_m + (x_I - x_m)\left.\frac{\partial h}{\partial x}\right|_m + (y_I - x_m)\left.\frac{\partial h}{\partial y}\right|_m \qquad \text{Equation 6}$$

De Marsily (1986) showed that the gradients are independent of the location of point m and that they are constant along AB. This allows the rearrangement of the left-hand side of Equation 5 by writing the head gradients outside the integrals. This greatly reduces the mathematical procedure required to carry out the integration and yields a relatively simple form as given in Equation 7.

$$\int_{AB} \left(T_x \frac{\partial h}{\partial x} n_x + T_y \frac{\partial h}{\partial y} n_y \right) ds = C_{IJ}\left(H_J - H_I\right) + C_{IK}\left(H_K - H_I\right) \qquad \text{Equation 7}$$

C_{IJ} and C_{IK} are constants that depend on the aquifer characteristics, specifically the transmissivity and the dimensions of the mesh. Equation 7 shows that integrated finite differences lead to an expression for flow in the form of head differences multiplied by constants. This is similar to the structure in conventional finite difference formulae. In addition, the method maintains both a flow balance and the reciprocity requirement. However, it also generates a high truncation error.

In conventional finite differences, the truncation error resulting from the calculation of $\frac{\partial h}{\partial x}$ or $\frac{\partial^2 h}{\partial x^2}$, using the central difference scheme, is in the order of O(Δx^2). The approach used by De Marsily results in an error in the order of O(Δx) for the calculation of $\frac{\partial h}{\partial x}$ or $\frac{\partial h}{\partial y}$. De Marsily et al. (1978) recognised that a model based on this approach does not represent the system accurately and De Marsily (1986) restricted the refinement by halving the mesh interval to maintain accuracy. This makes other refinement approaches such as the one developed by Jackson (2000) more desirable, even without maintaining reciprocity, since they produce better quality results.

The New Formulation

De Marsily et al. (1978) described their work as having a “logical synthesis” and as being “hydrogeologically plausible”. Indeed, integrated finite differences fit neatly with conventional finite differences and keep important features such as providing clear discretised aquifer units, maintaining a flow balance, and dealing with heterogeneous aquifers. However, the major problem with the method, as represented by De Marsily et al (1978) and De Marsily (1986), is the limited accuracy. To overcome this difficulty, a new formulation for the head gradients $\frac{\partial h}{\partial x}$

and $\frac{\partial h}{\partial y}$ is developed. Like De Marsily et al. (1978) it is based on using Taylor's series at selected grid nodes but it includes additional terms in the expansion.

There are three main challenges to this approach. The first is that the approximations become large and a tidy outcome where the fluxes consist of expressions composed of head differences multiplied by constants is not guaranteed. Second, the head gradients depend on the position of the point m as it moves along the interface and this complicates the integration to determine the flow. Finally, the equations must produce an accurate solution.

To increase the accuracy of the head gradient approximation to the order of $O(\Delta x^2)$ three extra terms of Taylor's series involving the terms $\frac{\partial^2 h}{\partial x^2}$, $\frac{\partial^2 h}{\partial y^2}$ and $\frac{\partial^2 h}{\partial x \partial y}$ are included in the head equation at a given node in addition to the three used by De Marsily et al. (1978) and shown in Equation 6. The calculation of the values of these six terms necessitates the application of Taylor's series at six nodes. However, the locations of these nodes define the structure of the equations. It is, therefore, preferable to arrange the nodes carefully in a definite geometrical layout so the mathematical manipulation is reduced. Two possible grid layouts for the refinement scheme are presented here. The first is similar to the one implemented by Jackson (2000) and is illustrated in Figure 2. This layout consists of a coarse grid with a refined region giving elongated rectangular flow interaction areas at the mesh interface.

For a typical node, I, on the fine-coarse interface, there are three sides of the flow interaction area , AB, BC and AD that require a new formulation of the head gradient, $\frac{\partial h}{\partial x}$ or $\frac{\partial h}{\partial y}$, while on the fourth side, CD, the conventional finite difference expression can be applied. Many problems arise in this case, especially along the sides BC and AD. Along segment BC for example, the determination of the hydraulic gradient $\frac{\partial h}{\partial y}$ requires two different evaluations, one along BE and the other along EC. The same is true for the determination of $\frac{\partial h}{\partial y}$ along AD. A second more serious problem concerns the water balance. Line AF, for example, represents a common boundary between nodes K and I. For the flow balance at node K, the expression for $\frac{\partial h}{\partial y}$ is based on head values at points L, I, K, R and J. When considering node I, the gradient is based on head values at points L, N, I, K, and J. In theory the two expressions should produce the same results, but because of the truncation errors this is not guaranteed. In general, the use of different combinations of head values will lead to inconsistent estimates of flow across a common boundary.

The second layout divides the coarse grid into a number of discrete areas for which flow balances are calculated. In this case, the areas can extend beyond the original coarse grid lines, as shown in Figure 3. This eliminates the elongated areas and ensures that all nodes in all meshes have a square or a rectangular shape with an aspect ratio similar to that of the coarse grid. The advantage of this arrangement is that for all the nodes located on the interface, there is only a need to derive one expression for one head gradient, either $\frac{\partial h}{\partial x}$ or $\frac{\partial h}{\partial y}$ depending on the direction of the node face.

In the new scheme groundwater heads at the six points I, K, J, L, N and P, shown in Figure 3, are expressed by Taylor's expansions based on a point m that is moving along the line AB. Equation 8 shows the expression for Node I; the heads at the other nodes take the same form.

$$h_I = h_m + (x_I - x_m)\left.\frac{\partial h}{\partial x}\right|_m + (y_I - y_m)\left.\frac{\partial h}{\partial y}\right|_m + \frac{(x_I - x_m)^2}{2!}\left.\frac{\partial^2 h}{\partial x^2}\right|_m + \frac{2}{2!}(x_I - x_m)(y_I - y_m)\left.\frac{\partial^2 h}{\partial x \partial y}\right|_m$$
$$+ \frac{(y_I - y_m)^2}{2!}\left.\frac{\partial^2 h}{\partial y^2}\right|_m$$

Equation 8

This equation was used by Quandalle and Franlab (1985) who built a numerical model with composite grids. However, they considered refinement in one direction only and estimated the hydraulic gradient at a single node at the mid-point of line AB. They did not derive a general expression for the hydraulic gradient and integrate it along the interface.

The next stage consists of solving the six equations containing values of six unknown head and head gradients to evaluate the hydraulic gradient $\frac{\partial h}{\partial x}$. This yield Equation 9:

$$M\frac{\partial h}{\partial x} = C_1(h_L - h_I) + C_1(h_J - h_I) + (C_2 + C_{10}C_7 + y_m C_{10}C_6)(h_L - h_J) + C_4(h_P - h_I)$$
$$+ (C_3 + C_5 + C_9 C_7 + y_m C_9 C_6)(h_K - h_I) + C_5(h_N - h_I) + (C_5 + C_8 + y_m C_8 C_6)(h_N - h_I)$$

Equation 9

Where:

$$M = \frac{-3\Delta x - \Delta X}{4\Delta x}$$

$$C_1 = \frac{-1}{\Delta x + \Delta X}, \qquad C_2 = \frac{-(2y_I - y_L - y_J)}{2\Delta Y(\Delta x + \Delta Y)}, \qquad C_3 = \frac{-(2y_I - y_L - y_J)}{2\Delta y(\Delta x + \Delta X)}$$

$$C_4 = \frac{-(\Delta x - \Delta X)}{4\Delta x^2}, \qquad C_5 = \frac{[(2y_I - y_L - y_J)\Delta y - \Delta Y^2]}{4\Delta y^2(\Delta x + \Delta X)}$$

$$C_6 = \frac{-(3\Delta x^2 + \Delta X^2 + 4\Delta x \Delta X)}{4\Delta x(\Delta x + \Delta X)}, \qquad C_7 = \frac{[(\Delta x + \Delta X)(y_I(\Delta x + \Delta X) + (y_I + y_L)\Delta x)]}{4\Delta x(\Delta x + \Delta X)}$$

$$C_8 = \frac{(y_I + y_N - y_L - y_J - 2\Delta y)}{\Delta y^2(\Delta x + \Delta X)}, \qquad C_9 = \frac{(y_I + y_N - y_L - y_J)}{\Delta y^2(\Delta x + \Delta X)}, \qquad C_{10} = \frac{2}{\Delta Y(\Delta x + \Delta X)}$$

Where Δx and Δy are the grid intervals on the fine grid and ΔX and ΔY are the corresponding values on the coarse grid as shown in Figure 3. Integrating Equation 9 over the interval AB and multiplying by the transmissivity in the x direction, gives the flow across AB. In the case of node I shown in Figure 3, the integration is carried out in the y direction. This only affects the variable y_m in Equation 9, since all other terms are independent of the position of m. The integration results in multiplying all terms that do not include y_m by Δy and in replacing y_m , by $\frac{1}{2}\left(y_B^2 - y_A^2\right) = y_I \Delta y$. The flow equation becomes:

$$Q_{AB} = \frac{T\Delta y}{M}\left[\begin{aligned} &C_1(h_L - h_I) + C_1(h_J - h_I) + (C_2 + C_{10}C_7 + P\cdot C_{10}C_6)(h_L - h_J) + C_4(h_P - h_I) \\ &+ (C_3 + C_5 + C_9C_7 + P\cdot C_9C_6)(h_K - h_I) + C_5(h_N - h_I) + (C_5 + C_8 + P\cdot C_8C_6)(h_N - h_I)\end{aligned}\right]$$

Equation 10

The symbol P in Equation 10 is used to indicate a term which changes for certain nodes. In general P is equal to y_I. The value changes when nodes fall along the line of the original coarse grid. Node N in Figure 3 represents one such node where the integration of Equation 9 over the interval BF is achieved in two steps. The first integral occurs over BE using head values located below the line LN while the second occurs over EF and uses head values located above LN. In both cases the equations are based on the hydraulic characteristics of node N and are similar to Equation 10. However, for the flow moving across segment BE, the value of P is adjusted to: $\left(y_N - \frac{\Delta y}{4}\right)$ and across EF the value of P is: $\left(y_N + \frac{\Delta y}{4}\right)$. With these modifications, Equation 10 is a general equation that takes a desirable numerical form of head differences multiplied by constants and it can be applied at all nodes along the grid interface.

The corresponding equations for interfaces oriented in decreasing x, and increasing and decreasing y directions can be obtained by careful re-arrangement of Equation 10. An example of this treatment can be found in Jackson (2000).

One slight problem arises at the extremities of the expanded mesh. The procedure does not allow the determination of groundwater head at nodes located at the corners of a child grid. This arises from the need for six points to calculate the flow balance as demonstrated for node I in Figure 4. For a point such as C in Figure 4, which is located at the corner of the child grid, the sixth node required for the calculation of the flow across DE is missing. To overcome this difficulty a virtual node is introduced beyond the extreme corner of a fine mesh. The head value at this extra node has to be estimated by interpolation.

Convergence of the Numerical Scheme

Convergence to steady state conditions

A first check on the new refinement scheme is to examine a simple steady state problem. This consists of a 2.5 km square aquifer, refined as shown in Figure 5a. The parent and the child grids are composed of 500 m and 100 m square cells respectively. The child grid lies at the middle of the coarse grid and both have the same transmissivity values of 100 m^2 day^{-1}.

Successive Over Relaxation (SOR) is used to solve the numerical system. SOR is a point iterative approach based on the Jacobi and the Gauss-Seidel iteration methods to solve a system of linear equations. The allowable error, representing the maximum flow imbalance at each node and at which the SOR procedure terminates, is set to a very small value of 1×10^{-8} m^3 day^{-1}. The head values generated by the model fit the analytical solution with maximum differences between the results of the analytical and numerical solutions not exceeding 0.15%. In this special case the interpolation technique calculates the groundwater heads at the missing nodes and the groundwater heads at the extreme ends of the child grid. The flows calculated by the model confirm that no flow is generated in the y direction and that the flow in the x direction is equal to that calculated using the analytical solution. This is an important check of the coding of the model because it confirms the correct implementation of the various forms of the refined area equations as well as the proper linkage between the different types of node.

The boundary conditions are specified as fixed head values on all sides and zero groundwater heads are specified everywhere as initial condition. A curved surface is created by introducing an abstraction well approximately in the centre of the child grid at the location labelled Node C in Figure 5a.

The numerical solution resulting from the proposed refined grid is compared to that produced using a regular fine mesh grid having 100 m square cells over the whole aquifer. After a certain period of continuous abstraction at a rate of 1000 m^3 day^{-1}, a steady state condition is reached. Figure 5b shows the contour lines resulting from both grids. The results are in close agreement and the contour lines of both solutions almost coincide. However, a closer examination reveals that some differences in head exist, reaching at certain locations an absolute value of 1.4%. This behaviour becomes clearer when the difference between the two solutions at the child grid boundary is examined. Since a line of symmetry crosses the aquifer diagonally, as shown in Figure 5a, only the upper and the lower faces of the child grid need be considered. Figure 6 shows the absolute head difference along these two boundary lines. The head difference varies from a minimum of 0.1% to a maximum value of 1.4% with the maximum difference located at the node opposite the abstraction point. The flow crossing the coarse-fine interface at the nodes common to both models is also compared in Figure 6. The absolute percentage difference in flow ranges from a minimum of zero to a maximum of 5.0%. It is clear that a small error in the computed head leads to a larger error in the flow. Reciprocally, a relatively large error in the flow may lead to insignificant differences in the corresponding head values. This is the main reason for basing the convergence criterion on an accurate determination of flow, i.e. minimising the flow imbalance, which certainly leads to an accurate head determination. This is also an advantage of the integrated finite difference refinement method which relies on the calculation of flow as a means of to determining head at the coarse-fine interface and not vice versa.

Reproducing time variant groundwater heads

Theis' (1935) analytical solution is used to investigate the capability of the new refinement scheme to produce the groundwater flow solution under time variant conditions. Groundwater flows are simulated in a large 10 km square aquifer with fixed heads at its outer boundaries. Large dimensions of the aquifer are necessary to reduce the interference of the outer boundaries with the numerical results, especially at the later times of the simulation. the transmissivity of the aquifer is set to a value of 100 m^2 day^{-1} and the storage coefficient is set to a value of 0.0001. To satisfy the Theis assumptions, no recharge is applied, the initial head values are set to zero, i.e. no drawdown occurs at time zero, and the abstraction increases instantaneously to the rate of 1000 m^3 day^{-1}. Finally, to allow a small nodal area at the abstraction borehole so that it resembles an infinitely small well, the aquifer is refined in three stages; at the coarsest level, a grid with 500 m square cells is used, followed by a grid with 100 m square cells as an intermediate stage and finally a grid with 20 m square cells is used for the finest mesh. These settings are shown in Figure 7.

Time drawdown curves generated by the model are compared to the Theis solution at three observation wells. The locations of the observation (Figure 7) wells are selected to show groundwater head values calculated at nodes located on the three grids. The distances between the observation boreholes and the abstraction borehole are 141 m, 500 m and 1500 m. Figure 8 shows the simulated time drawdown curves and those produced using the Theis solution. It is clear that there is good agreement between these curves except at the early times of pumping. The disparity between the results is attributed to the difference in the representation of the sink in the numerical model and it representation as a line source in the Theis analytical solution. After day 7 the outer boundary effects start to appear in the simulated results. This is reflected by the reduction of the gradient of the time drawdown curves indicating that some water is being supplied by the outer fixed head nodes to the pumped borehole.

Simulation of groundwater heads in heterogeneous aquifers

The presented numerical scheme can be readily used to simulate groundwater heads in heterogeneous aquifers on condition that the transmissivity value specified at one coarse grid node is the same as the transmissivity values of the child nodes in contact with it. Reproducing the groundwater heads in heterogeneous aquifers is tested in this section.

An aquifer that is 5 km long and 2.5 km wide with a global transmissivity value of 100 m2 day-1 and a storage coefficient value of 0.0001 is discretised using a grid with 500 m square cells, which is refined at its centre as illustrated in Figure 9a. The refining grid has 100 m square cells. The aquifer has zones with transmissivity values of 50 and 200 m2 day-1 as shown in Figure 9a. The aquifer has fixed head boundaries along its sides, has no recharge and is pumped at a rate of 1000 m3 day-1 at its centre. Figure 9b shows the groundwater head contour lines produced from this model and those produced from a model using a fine with 100 m square cells after a simulation time of 10 days. These contours are in close agreement with the observed discrepancy related to contouring artefact. A closer comparison between the simulated results shows that the overall discrepancy is ranging between 3 and 5% but with few cells showing high error values of up to 13%. While the latter error figure recommends further investigations into its source, the cells associated with it are located next to the fixed head boundaries. The groundwater heads calculated at these cells are in the order of 10 cm while the highest drawdown values calculated at the centre is 1%.

Discussion and Conclusion

The refinement scheme is based on the integrated finite differences approach. It is similar to that used by De Marsily et al. (1986) as it relies on the divergence theorem and Taylor's expansions. The divergence theorem is used to transform a double integral of the basic flow equation over the area associated with a node into a contour integral around the perimeter of this same area. Taylor's expansions are used to determine the hydraulic gradient along the perimeter. The accuracy of the developed numerical equations is improved by including terms up to the second order from the Taylor's expansions. This is the main difference from the work presented by De Marsily et al. (1986); however, the inclusion of these additional terms requires extra mathematical computation to derive the numerical equations that describe the flow across the fine-coarse mesh interface. Significantly, the new flow equations maintain the desired form, which calculates the flow as the product of head differences multiplied by a constant as in the conventional finite difference formulae.

The numerical grid layout used to refine the grid affects the difficulties associated with producing the numerical equations. It has been found that dividing the nodes rather than the mesh increases the number of sides over which the conventional finite difference equations are applied, and increases the accuracy of the model. The derived numerical equations converged to the required solution without difficulty, although in some cases the over relaxation factor had to be limited to values less than 1.4 to ensure the convergence of the solution.

The new refinement scheme is tested for its ability to represent the groundwater heads in homogeneous and heterogeneous aquifers under steady state and time variant conditions. The developed numerical technique relies on the principle of using the Taylor's series to calculate the groundwater head gradients at a point moving along a node face. This requires that the groundwater surface is continuous and differentiable between all the nodes in order to calculate the gradient at that point. For a heterogeneous aquifer, the refining grid must be selected such that the aquifer does not change in its properties between the nodes surrounding the point where the hydraulic gradients are calculated

Accurate results were generated for a drawdown surface that curves in one direction only. However, the technique generated undesirable but small errors in the representation of a drawdown surface that curves in two directions. These errors arise because of the interpolation necessary to calculate head values at the imaginary nodes at the corners, which are required to comply with the new formulae. However, the differences between the numerical results and the analytical results fall within an acceptable range. The flow errors are found to be higher than the head errors; this is expected since a very small change in the head values can lead to relatively high changes in water flows. It is therefore much better to stop the iteration process in the numerical model when it attains an acceptable water balance rather than when the heads stop changing significantly. This is where the integrated finite difference approach, where the calculation of flows at all node faces is possible, prevails over other refinement schemes.

This refinement scheme shows the potential of having more advantages than other refining techniques so far reported in the literature. For example, the order of refinement can be increased to order of refinement higher than 5, the limit imposed by Jackson (2000) on his refinement technique. This refinement approach together with the layout of the grid described in this paper also offers the possibility of setting a concave refinement configuration, i.e. when the part of the child grid takes an L shape. In addition, the integrated finite difference application presented here can be applied to non-linear grid interface. This opens the possibility of deriving groundwater flow equations to nodes located at the edges of a cylindrical grid model and consequently embedding the cylindrical grid model in a Cartesian model. This investigation is ongoing.

References

Arney, D.C., and Flaherty J.E. 1989. An adaptive local mesh refinement method for time-dependent partial differential equations. *Applied Numerical Mathematics*, 5, 257-274.

Bennett B.A.V., and Smooke M.D. 1999. Local rectangular refinement with application to nonreacting and reacting fluid flow problems. *Journal of Computational Physics*, 151, 684-727.

Berger M.J., and Oliger J. 1984. Adaptive mesh refinement for hyperbolic partial differential equations. *Journal of Computational Physics*, 53, 484-512.

Boas M.L. 1983. *Mathematical methods in the physical sciences*. New York: John Wiley and Sons.

Bravo R., Rogers J.R., and Cleveland T.G. 1996. Modelling groundwater flow using flux boundary conditions. *Water Resources Bulletin*, 32, 1, 39-46.

De Lange H.C., and De Goey L.P.H. 1994. Numerical flow modelling in a locally refined grid. *International Journal for Numerical Methods in Engineering*, 37, 487-515.

De Marsily G., Ledoux E., Levassor A., Poitrinal D., and Salem A. 1978. Modelling of large multilayered aquifer systems: Theory and applications. *Journal of Hydrology*, 36, 1-34.

De Marsily G. 1986. *Quantitative Hydrogeology*. San Diego: Academic Press.

Dickinson E.J., James S.C., Mehl S., Hill M.C., Leake S.A., Zyvoloski G.A., Faunt C.C., and Eddebbarh A. 2007. A new ghost-nod method for linking different models and initial investigations of heterogeneity and nonmatching grids. *Advances in Water Resources*, 30, 1722-1736.

Diersch H.j.G. 2005. FEFLOW finite element subsurface flow and transport simulation system reference manual. WASY GmbH Institute for Water Resources planning and Systems Research. Berlin

Hayes P.J. 1999. An r-theta co-ordinate numerical model, incorporating mesh refinement, for the investigation of pumping tests in heterogeneous aquifers. Ph.D. Thesis, The University of Birmingham, Birmingham, U.K.

Jackson J.R. 2000. A novel grid refinement method for regional groundwater flow using Object Oriented technology. Ph.D. Thesis, The University of Birmingham, Birmingham, U.K.

Mansour M.M., Hughes A.G., Spink A.E.F., Riches J. 2011. Pumping Test Analysis Using a Layered Cylindrical Grid Numerical Model in a Complex, Heterogeneous Chalk Aquifer. *Journal of Hydrology*, 1-2, 14 – 21.

Mehl S., and Hill M.C. 2004. Three-dimensional local grid refinement for block-centered finite-difference groundwater models using iteratively coupled shared nodes: a new method for interpolation and analysis of errors. *Advancs in Water Resources*, 27, 899 – 912.

Mehl S., Hill M.C., and Leake A.A. 2006. Comparison of local grid refinement methods for MODFLOW. *Ground Water*, 44, 6, 792 – 796.

Miller R.T. and Voss C.I. (1987). Finite-difference grid for a doublet well in an anisotropic aquifer. Ground Water, 24, 4, 490-496

Quandalle P. and Franlab P.B. 1985. Reduction of grid effects due to local sub-gridding in simulations using a composite grid.

Rushton K. R. And Redshaw S.C. 1979. *Seepage and groundwater flow*. Chichester : Wiley.

Southwell R.V. 1946. *Relaxation methods in theoretical physics*. Oxford : Clarendon Press.

Szekely F. 1998. Windowed spatial zooming in finite-difference ground water flow models. *Ground Water*, 36, 5, 718-721.

Szekely F. 2008. Three-dimensional mesh resolution control in finite difference groundwater flow models through boxed spatial zooming. *Journal of Hydrology*, 351, 261-267.

Theis C.V. 1935. The relation between the lowering of the piezometric surface and the rate and duration of discharge of a well using ground-water storage. *Transactions of the American Geophysical Union*, 16th annual meeting, 519-524.

Ward D.S., Buss D.R., Mercer J.W., and Hughes S.S. 1987. Evaluation of groundwater corrective action at the Chem-Dyne hazardous waste site using a telescopic mesh refinement modeling approach. *Water Resources Research*, 23, 4, 603-617.

Zzvoloski G.A., Robinson B.A., Dash Z.V., and Trease L.L. 1997. Summary of the models and methods for the FEHM application: A finite-element heat- and mass-transfer code. Los Alamos National Laboratory Report LA-13306-MS.

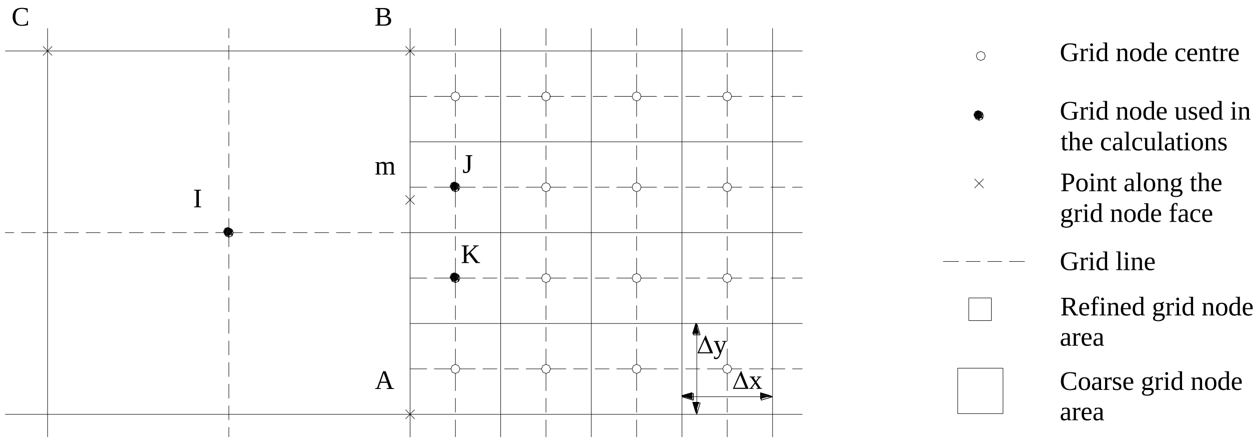

Figure 1: Parent-Child grid interface in a refined grid

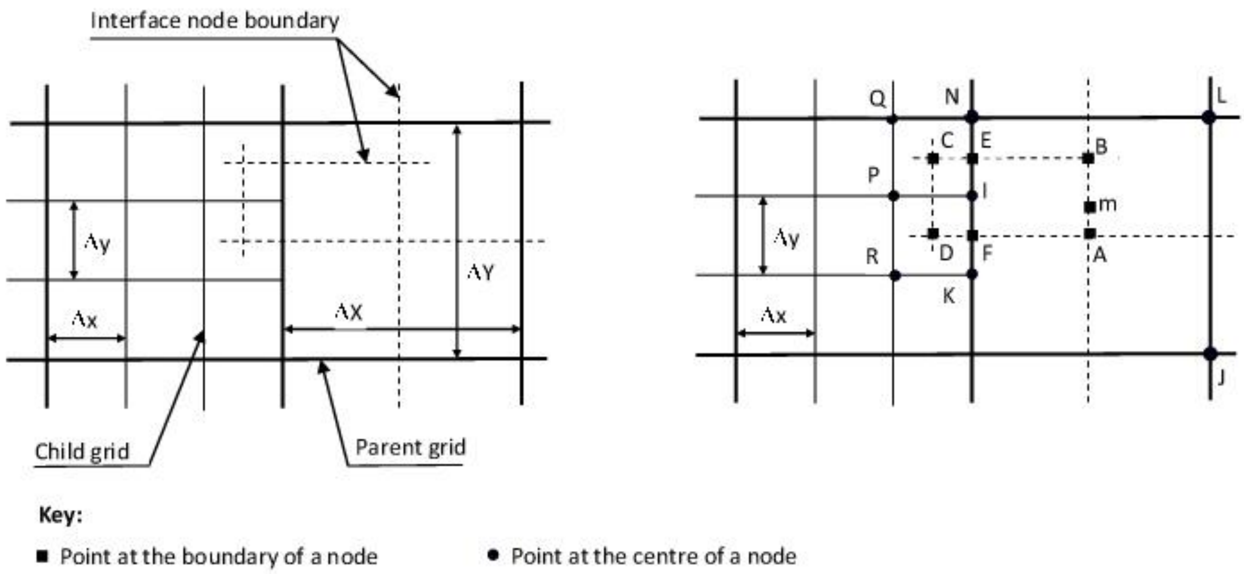

Figure 2: Grid layout proposed by Jackson (2000).

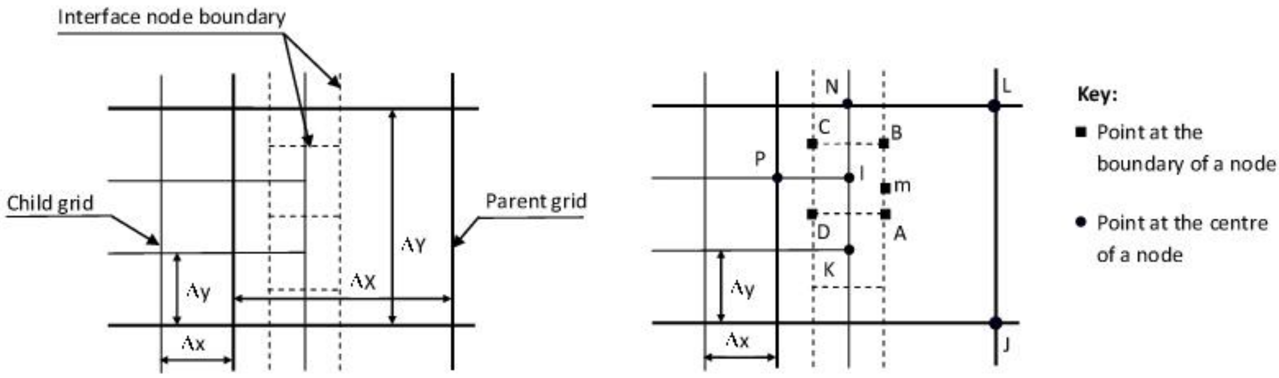

Figure 3: The new grid layout used to derive the numerical expressions

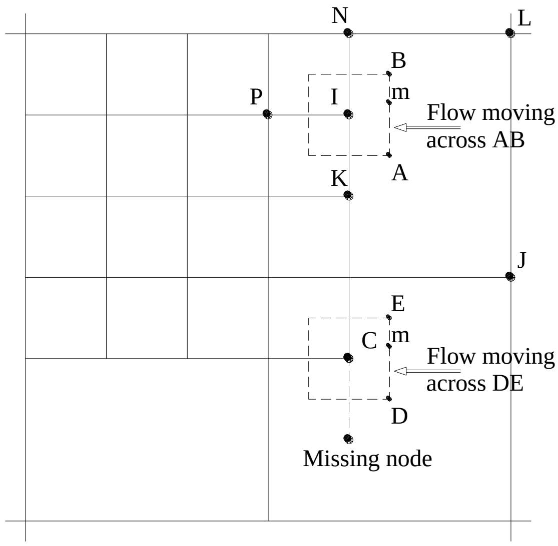

Figure 4: An imaginary node replaces the missing node adjacent to the corner node.

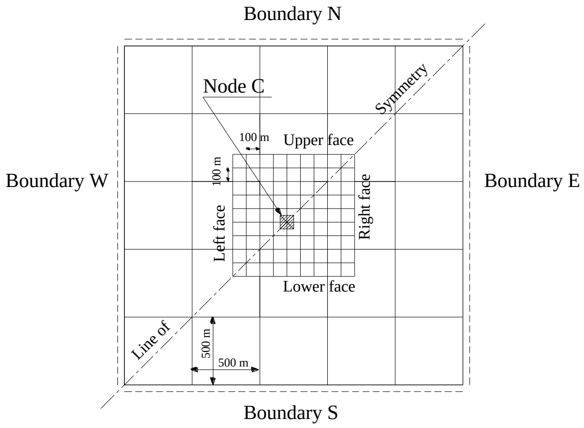

Figure 5: Refined grid representing a homogenous aquifer.

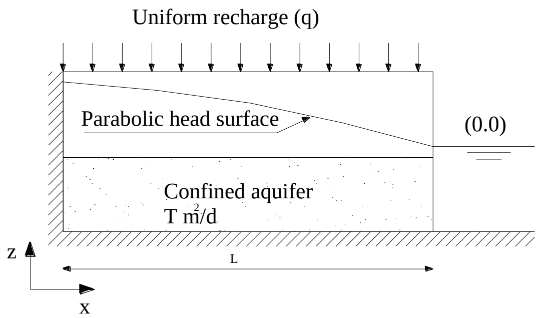

Figure 6: One dimensional representation of a homogeneous aquifer subjected to uniform recharge.

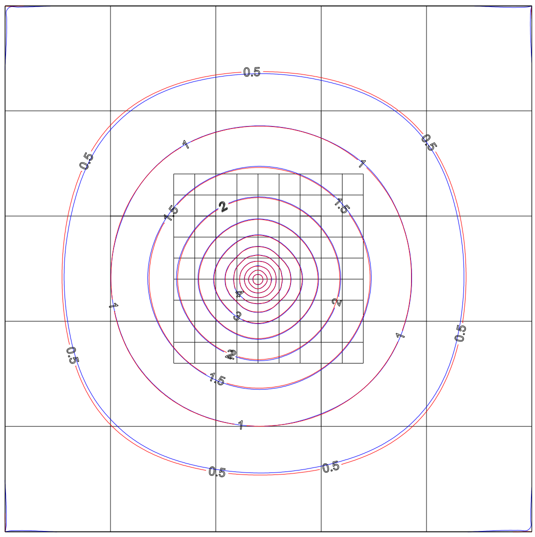

Figure 7: Contour lines resulting from a model with a refined grid (blue line) and a regular fine mesh (red line)

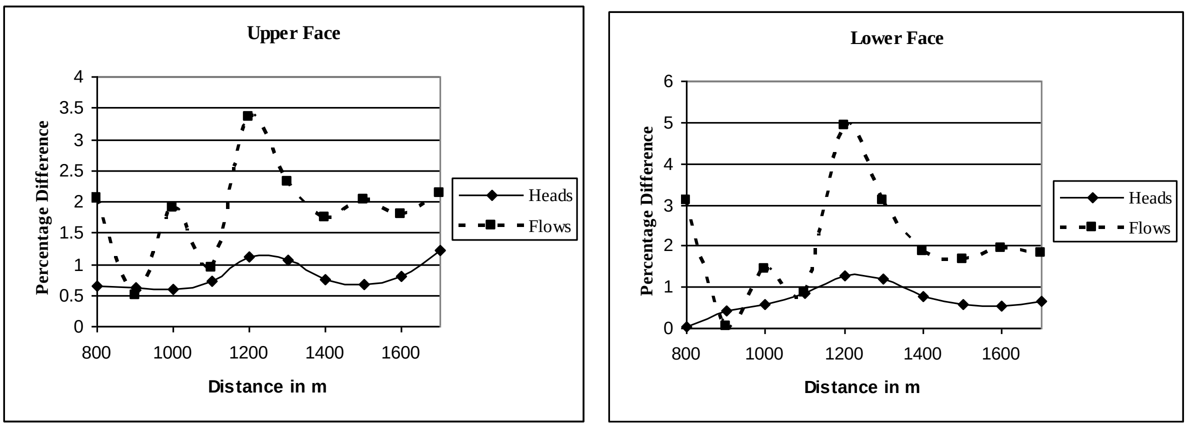

Figure 8: Absolute percentage flow and head differences at nodes located on the left and upper sides of the child grid.

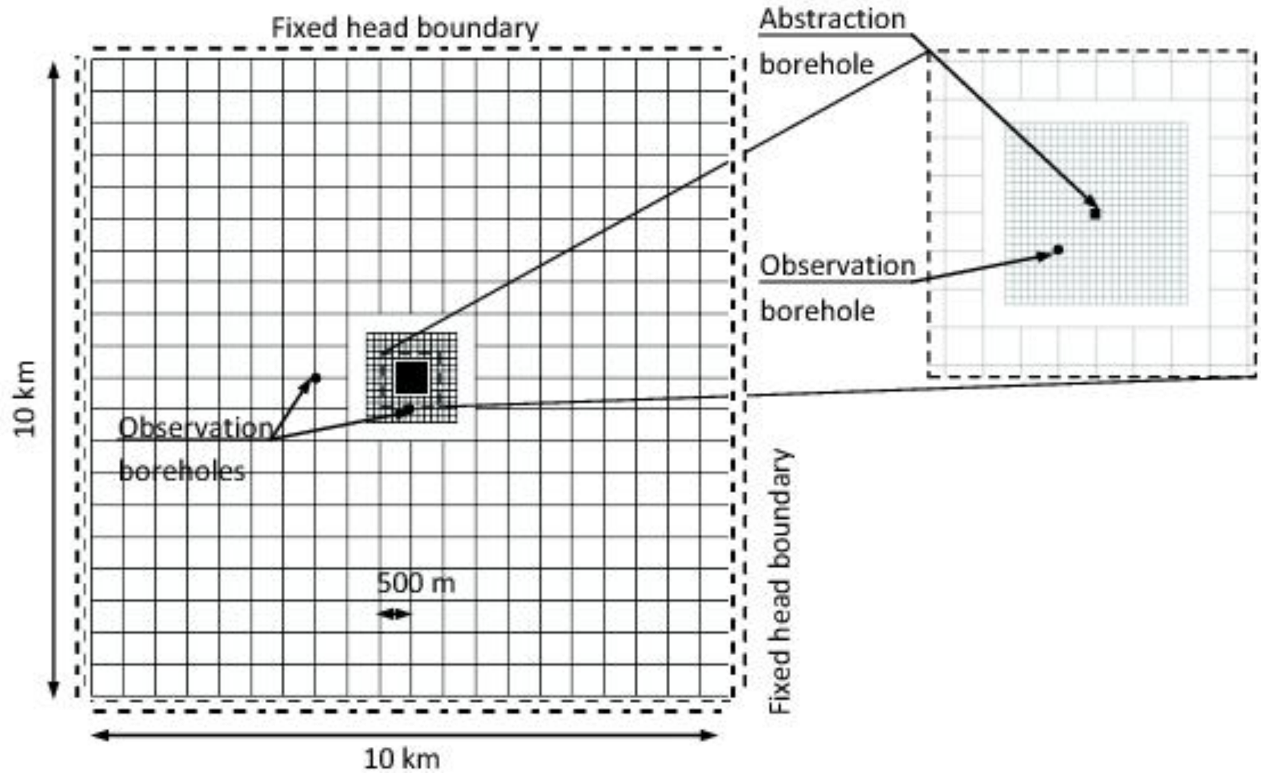

Figure 9: Three levels of refinement in a homogeneous aquifer subject to pumping.

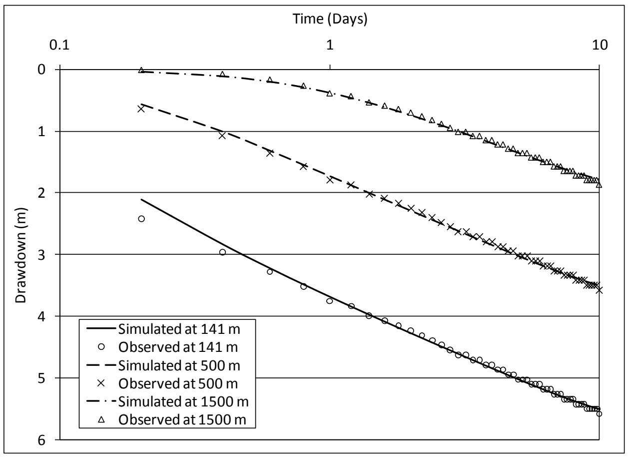

Figure 10: Comparison between simulated time drawdown curves and the Theis solution at observation boreholes located at 100 m, 500 m and 1500 m from the abstraction borehole.